HTML ABSTRACT + LINKS

Photonic band gaps and defect modes of polymer photonic crystal slabs

Chul-Sik Kee[a)]
Advanced Photonics Research Institute, Gwangju Institute of Science and Technology, Gwangju 500-712, Korea and Optical Interconnection Team, Basic Research Laboratory, Electronics and Telecommunications Research Institute, Daejeon 305-350, Korea

Sang-Pil Han, Keun Byoung Yoon, Choon-Gi Choi, and Hee Kyung Sung
Optical Interconnection Team, Basic Research Laboratory, Electronics and Telecommunications Research Institute, Daejeon 305-350, Korea

Sang Soon Oh and Hae Yong Park
Department of Physics, Korea Advanced Institute of Science and Technology, Daejeon 305-701, Korea

Sunggook Park and Helmut Schift
Laboratory of Micro and Nanotechnology, Paul Scherrer Institute (PSI), CH-5232, Villigen PSI, Switzerland

(Received 30 July 2004; accepted 2 December 2004; published online 24 January 2005)

We show from the photonic band calculation and the finite difference time domain simulation that polymer photonic crystal slabs with a triangular array of air holes can exhibit complete photonic band gaps for transverse electric-like modes. A line defect introduced in the polymer photonic crystal slab can create guided modes which are useful in implementing low loss waveguides. We also show that thermal nanoimprint lithography is an attractive way to pattern the triangular array of air holes with high aspect ratio, which is a necessary step in the realization of the polymer photonic crystal slab. © *2005 American Institute of Physics*. [DOI: 10.1063/1.1857069]

Photonic crystals exhibit many interesting properties such as photonic band gap (PBG), i.e., the frequency range where electromagnetic waves cannot propagate in any direction, and defect modes, i.e., the allowed modes in the PBGs introduced by local defects in the photonic crystals.[1–3] The electromagnetic field of a defect mode is, just as the wave function of a defect state is tightly localized around the defect in semiconductors, strongly localized around the local defect.[4] Thus a point (line) defect can act like a microcavity (waveguide).[5] Moreover, we can control the frequency of the defect mode by changing the size and shape of the defect. These controllable defect modes play key roles in the applications of photonic crystals in optical microcavities and waveguides.[6–8]

Of various structures that have been proposed for photonic crystals, photonic crystal slabs which are high dielectric slabs with a two-dimensional array of air holes on low dielectric substrates have been intensively investigated since they can be fabricated at telecommunication wavelengths using semiconductor technologies and give an opportunity to control the propagation of light in-plane.[9] By incorporating structural defects such as point or line defects into photonic crystal slabs, various functional optical components can be implemented. Thus they are expected to serve as new platforms for planar photonic integrated circuits (PICs).

Conventional planar PICs have been developed using low dielectric materials such as polymers since these materials show low propagation loss at telecommunication wavelengths and are compatible with optical fibers.[10] Thus, if polymer slabs with two-dimensional periodic patterns, namely polymer photonic crystal slabs, can exhibit PBGs, they can be attractive candidates for platforms implementing low loss PBG PICs. The previous works, however, have shown that polymer photonic crystal slabs exhibit *incomplete* in-plane PBGs and they are not suitable for the implementation of waveguides and cavities which play key roles in the PBG functional devices.[11–13]

In this letter, we show that a polymer slabs suspended in air with a triangular array of air holes can exhibit a *complete* band gap for transverse electric (TE)-like modes whose magnetic field is parallel to the axis of hole and symmetric to the horizontal plane bisecting the slab. The simulated transmission spectra for the modes propagating along the ΓK and ΓM directions of the triangular lattice show a common stop band range which agrees well with the region of the band gap obtained by the photonic band calculation. We also show that reduced width-line defects can create defect modes that are useful in the implementation of low loss PBG waveguides. In addition, we show that photonic crystal structures can be fabricated using nanoimprint lithography (NIL), by molding a regular array of holes into a thin thermoplastic polymer layer.

We consider polystyrene as a suitable polymer material because it can be molded due to its low glass transition temperature ($T_g = 90\ ^\circ\mathrm{C}$) and its refractive index ($n = 1.59$) is rather larger than those of other polymers used in optical devices. The conjugate gradient plane wave expansion method[14] was employed to calculate the photonic band structures of the polymer slab with a triangular array of holes. The transmission spectra were simulated using the three-dimensional finite difference time domain method.[15]

Figure 1 shows the photonic band structure for TE-like modes of the polystyrene photonic crystal slab assuming the thickness of the slab $t = 1.2a$ and the hole radius $R = 0.34a$, where a is the lattice constant. The frequency is normalized to $2\pi c/a$, where c is the light speed in vacuum. The solid line is the light line and thus the gray region denotes radiation modes that can be coupled with free space modes. The inset indicates the points of high symmetry in the first Bril-

[a)]Author to whom correspondence should be addressed; electronic mail: cskee@gist.ac.kr

 © 2005 American Institute of Physics
Downloaded 20 Apr 2011 to 143.248.103.111. Redistribution subject to AIP license or copyright; see http://apl.aip.org/about/rights_and_permissions

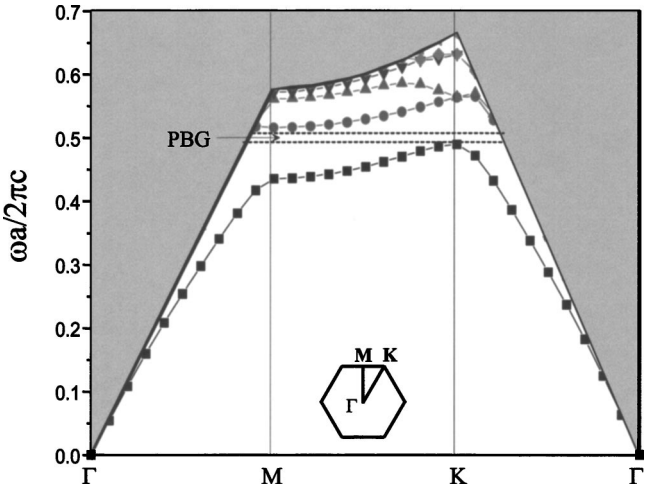

FIG. 1. Photonic band structure for the TE-like modes of polystyrene photonic crystal slab in air with a triangular array of air holes when the thickness $t=1.2a$ and the hole radius $R=0.34a$, where a is the lattice constant. The frequency is normalized to $2\pi c/a$, where c is the light speed in vacuum. The solid line is the light line. The inset indicates the points of high symmetry in the first Brillouin zone of triangular lattice.

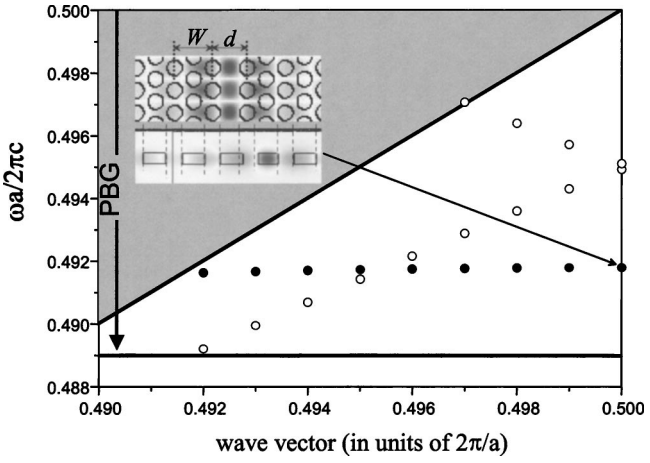

FIG. 3. Photonic bands of defect modes when the width of line defect $d=0.9W$, where W is the width of the line defect created by removing one line of holes in the ΓK direction. The closed (open) circles represent the defect modes with even (odd) parity which are symmetric (asymmetric) about the plane bisecting the line defect. The inset shows the field distribution for even mode at $k=0.5(2\pi/a)$.

louin zone of the triangular lattice. One can see that the polystyrene photonic crystal slab can exhibit a complete in-plane PBG between 0.49 and 0.51. Note that the upper edge frequency of the PBG is the intersection of light line and the second band of ΓK direction, not the frequency of the second eigenmode at M point. To confirm the narrow band gap, we have also calculated the transmission spectra for the TE-like modes propagating along ΓK and ΓM directions. Our calculation domain contained 13×22 unit cells and each unit cell was divided into $16\times16\times10$ discretization grid cells. The total number of time steps was 2^{16}, with each time step $\Delta t=\Delta x/(3c)$. The source was simulated as a Gaussian beam in time domain and in the coordinate space. Figure 2 shows the simulated transmission spectra for the TE-like modes propagating along ΓK (solid line) and ΓM (dashed line) directions assuming that the lattice constant of the triangular array is 775 nm and thus the diameter of hole $2R=527$ nm $(0.68a)$ and the thickness of the polystyrene slab $t=930$ nm $(1.2a)$.

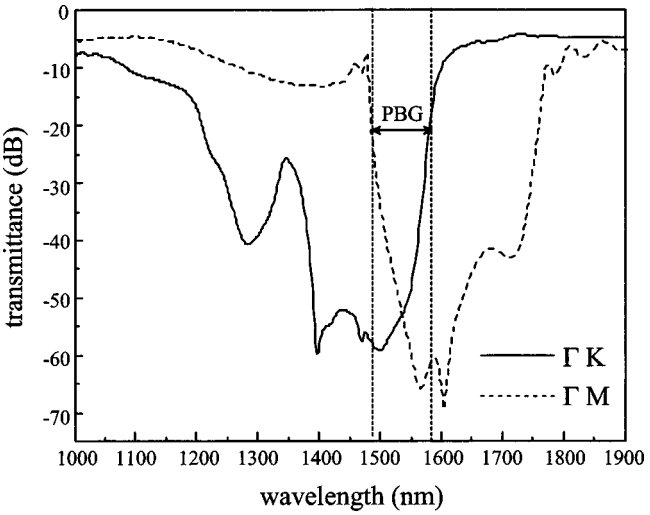

FIG. 2. Simulated transmission spectra for the TE-like modes propagating along ΓK (solid line) and ΓM (dashed line) directions when $a=775$ nm, $2R=527$ nm $(0.68a)$, and $t=930$ nm $(1.2a)$. The stop band range where the transmittance is lower than 20 dB is from 1500 to 1580 nm.

One can see the common stop band in the transmission spectra along the two directions. The stop band range where the transmittance is lower than 20 dB is from 1500 to 1580 nm. This agrees well with the band gap range between 1519 and 1581 nm, which was determined from Fig. 1.

It is worth investigating defect modes of line defects in the proposed polymer PBG structure since the defects have played key roles in the implementation of various functional PBG devices such as ultrasmall bending waveguides, power dividers, directional couplers, and so on. The supercell method was employed to calculate the photonic bands of defect modes introduced by line defects. Figure 3 shows the photonic bands when the width of line defect $d=0.9W$, where W is the width of line defect created by removing a line of holes in the ΓK direction. The closed (open) circles denote the defect modes with even (odd) parity which are symmetric (asymmetric) about the plane bisecting the line defect. The inset shows that the schematic of the line defect and the field distribution of the even mode at $k=0.5(2\pi/a)$. One can see that the field is strongly localized around the line defect, indicating a creation of guided modes propagating along the line defect. However, the band of even modes is so flat and thus the guided range is narrow and their group velocities are extremely small. These characteristics of the defect modes have already been experimentally observed in the silicon-on-insulator (SOI) PBG slab waveguides.[16] For practical applications, it is desirable to have a guided range of reasonable width and single modes with sufficiently large group velocity. Thus various ways have been recently proposed to achieve the desirable characteristics of SOI PBG slab waveguides.[17–19] We believe that the proposed methods can also be applicable to the polymer PBG slab waveguides.

Nanofabrication of low refractive index material films with one- or two-dimensional periodic patterns using parallel and low-cost techniques such as NIL recently has attracted considerable attention.[20,21] NIL has demonstrated to be suitable for patterning various polymers and, if used as a resist, these patterns can be transferred into inorganic materials. 150 mm wafers with feature sizes of 50 nm have been processed and passive optical devices for the infrared and visible wavelength ranges have been realized.[12,13] In realizing

Downloaded 20 Apr 2011 to 143.248.103.111. Redistribution subject to AIP license or copyright; see http://apl.aip.org/about/rights_and_permissions

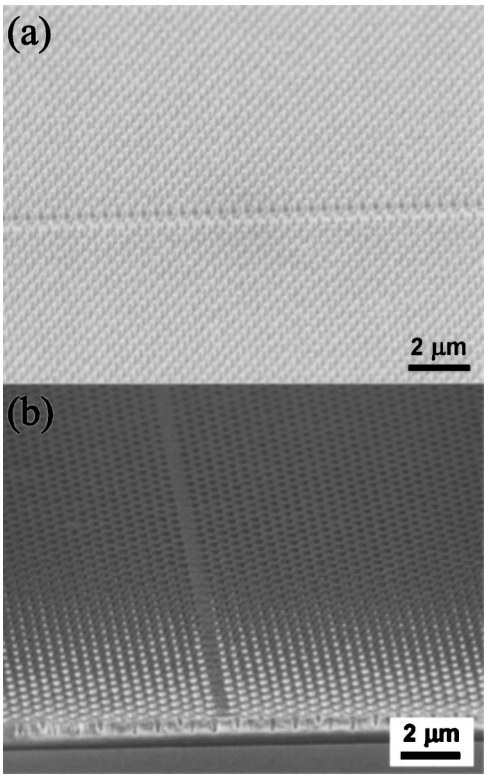

FIG. 4. Scanning electron microscopy micrographs of the silicon stamp having a triangular array of rods with a line defect fabricated using e-beam lithography and subsequent anisotropic reactive ion etching of silicon (a) and PMMA film imprinted by the stamp (b). The radius of rod is 130 nm and the lattice constant 405 nm. The averaged depth of imprinted holes measured by the atomic force microscopy is about 385 nm.

suspended polymer photonic crystal slabs, the difficulties lie in the fabrication of patterns with high aspect ratio in the polymer film because the choice of etch masks applicable to polymeric materials is very limited. As a means of overcoming this, we have employed NIL to emboss stamps with high aspect ratio lines and rod arrays into thin polymer films directly and to transfer these patterns into various materials.[22]

Figure 4(a) shows the scanning electron microscopy micrograph of the silicon stamp having a triangular array of circular rods with a line defect fabricated using e-beam lithography and subsequent anisotropic reactive ion etching of silicon. The radius of rod is 130 nm and the lattice constant 405 nm. We were able to imprint the silicon stamp with the rod height of 400 nm polymethylmethacrylate (PMMA) ($n=1.49$) film on the silicon substrate [Fig. 4(b)]. The averaged depth of imprinted holes measured by the atomic force microscopy is about 385 nm, which is a little bit lower than the rod height of the stamp. Patterning of higher aspect ratio structures may also be possible with optimized process parameters, better anti-adhesive layers and stamps with smoother side wall roughness. The dimensions of the fabricated structure are different from those of the proposed structure. However, NIL can easily be extended for patterns of the dimensions of the proposed structures. Thus, our results indicate that NIL can be a suitable method to fabricate the photonic crystals structures not only for the infrared but also for the visible region and even beyond. The fabrication of membranes suspended in air further requires one to remove the silicon substrate, which can be done by wet and dry etching methods. This process has already been demonstrated for thin nanostructured Si_3N_4 membranes with regular arrays of holes.[22] For the fabrication of polymeric membranes, as used for the photonic crystal slabs presented here, methods have to be found for the selective removal of the underlying substrate without damaging the polymer. Progress in this issue and the optical characterization of proposed photonic crystal structures will be reported in the future.

In summary, we showed theoretically that low refractive index polymer slabs with a triangular array of air holes can exhibit complete in-plane PBGs for the TE-like modes and the reduced width-line defects can introduce the guided modes propagating along the line defects. The successful embossing of a triangular array of rods into polymer film indicate that the nanoimprint process could be suitable for the fabrication of polymeric photonic crystal structures. Nanoimprinted polymer photonic crystal slabs will be useful in the implementation of low-cost and low-loss PBG optical devices.

This research was in part supported by a grant (Code No. 02-K-01-006-30) from Center for Nanoscale Mechatronics & Manufacturing, one of the 21st Century Frontier Research Programs, which are supported by Ministry of Science and Technology, Korea.

[1] E. Yablonovitch, Phys. Rev. Lett. **58**, 2059 (1987).
[2] S. John, Phys. Rev. Lett. **58**, 2486 (1987).
[3] E. Yablonovitch, T. J. Gmitter, and K. M. Leung, Phys. Rev. Lett. **67**, 2295 (1991).
[4] J. D. Joannopoulos, R. D. Meade, and J. N. Winn, *Photonic Crystals: Molding the Flow of Light* (Princeton University Press, Princeton, 1995), Chaps. 4 and 5.
[5] R. D. Meade, A. Devenyi, J. D. Joannopoulos, O. L. Alerhand, D. A. Smith, and K. Kash, J. Appl. Phys. **75**, 4753 (1994).
[6] S. Fan, P. R. Villeneuve, J. D. Joannopoulos, and H. A. Haus, Phys. Rev. Lett. **80**, 960 (1998).
[7] O. Painter, R. K. Lee, A. Scherer, A. Yariv, J. D. O'Brien, P. D. Dapkus, and I. Kim, Science **284**, 1819 (1999).
[8] S. Noda, A. Chutinan, and M. Imada, Nature (London) **407**, 608 (2000).
[9] See, for example, IEEE J. Quantum Electron. **38**, 726 (2001).
[10] G. Bottger, C. Liguda, M. Schmidt, and M. Eich, Appl. Phys. Lett. **81**, 2517 (2002).
[11] C. Liguda, G. Bottger, A. Kuligk, R. Blum, M. Eich, H. Roth, J. Kunert, W. Morgenroth, H. Elsner, and H. G. Meyer, Appl. Phys. Lett. **78**, 2434 (2001).
[12] J. Seekamp, S. Zankovych, A. H. Helfer, P. Maury, C. M. Sotomayor Torres, G. Bottger, C. Ligura, M. Eich, B. Heidari, L. Montelius, and J. Ahopelto, Nanotechnology **13**, 581 (2002).
[13] C. M. Sotomayor Torres, S. Zankovych, J. Seekamp, A. P. Kam, C. C. Cedeno, T. Hoffmann, J. Ahopelto, F. Reuther, K. Pfeiffer, G. Bleidiessel, G. Gruetzner, M. V. Maximov, and B. Heidari, Mater. Sci. Eng., C **23**, 23 (2003).
[14] R. D. Meade, A. M. Rappe, K. D. Brommer, and J. D. Joannopoulos, Phys. Rev. B **48**, 8434 (1993).
[15] K. S. Kunz and R. J. Luebbers, *Finite Difference Time Domain Method for Electromagnetics* (CRC Press, Boca Raton, FL, 1993).
[16] M. Notomi, A. Shinya, K. Yamada, J. Takahashi, C. Takahashi, and I. Yokohama, IEEE J. Quantum Electron. **38**, 736 (2001).
[17] K. Yamada, H. Morita, A. Shinya, and M. Notomi, Opt. Commun. **198**, 395 (2001).
[18] M. M. Sigalas and E. Chow, J. Appl. Phys. **93**, 10125 (2003).
[19] K. Hosomi and T. Katsuyama, IEEE J. Quantum Electron. **38**, 825 (2001).
[20] S. Y. Chou, P. R. Krauss, W. Zhang, L. Guo, and L. Zhuang, J. Vac. Sci. Technol. B **15**, 2897 (1997).
[21] R. W. Jaszewski, H. Schift, J. Gobrecht, and P. Smith, Microelectron. Eng. **41**, 575 (1998).
[22] L. J. Heyderman, B. Ketterer, D. Bachle, F. Glaus, B. Haas, H. Schift, K. Vogelsang, J. Gobrecht, L. Tiefenauer, O. Dubochet, P. Surbled and T. Hessler, Microelectron. Eng. **67**, 208 (2003).

Downloaded 20 Apr 2011 to 143.248.103.111. Redistribution subject to AIP license or copyright; see http://apl.aip.org/about/rights_and_permissions